Neoplasia 63 (2025) 101151

Contents lists available at ScienceDirect

Neoplasia

journal homepage: www.elsevier.com/locate/neo

Original Research

LSD1+8a is an RNA biomarker of neuroendocrine prostate cancer

Anbarasu Kumaraswamy [a,b,1], Rahul Mannan [c,d,1], Olivia A. Swaim [a,b,1], Eva Rodansky [a,b], Xiao-Ming Wang [c,d], Aaron Udager [c,d], Rohit Mehra [c,d], Hui Li [e], Colm Morrissey [f], Eva Corey [f], Michael C. Haffner [g,h,i], Peter S. Nelson [g,h,i], Arul M. Chinnaiyan [b,c,d,j,k], Joel A. Yates [a,b], Joshi J. Alumkal [a,b,d,*]

[a] *Department of Internal Medicine, University of Michigan, Ann Arbor, MI, USA*
[b] *Rogel Cancer Center, University of Michigan, Ann Arbor, MI, USA*
[c] *Department of Pathology, University of Michigan, Ann Arbor, MI, USA*
[d] *Michigan Center for Translational Pathology, University of Michigan, Ann Arbor, MI, USA*
[e] *RevMAb Biosciences, Burlingame, CA, USA*
[f] *Department of Urology, University of Washington, Seattle, WA, USA*
[g] *Division of Clinical Research, Fred Hutchinson Cancer Center, Seattle, WA, USA*
[h] *Division of Human Biology, Fred Hutchinson Cancer Center, Seattle, WA, USA*
[i] *Department of Laboratory Medicine and Pathology, University of Washington, Seattle, WA, USA*
[j] *Department of Urology, University of Michigan, Ann Arbor, MI, USA*
[k] *Howard Hughes Medical Institute, Ann Arbor, MI, USA*

ARTICLE INFO

Keywords:
LSD1+8a
Neuroendocrine Prostate Cancer
RNA Biomarker
RNA In Situ Hybridization

ABSTRACT

Background: Lysine-specific demethylase 1 (LSD1) is a histone demethylase and regulator of differentiation, including in cancer. A neuronal-specific isoform of *LSD1*—*LSD1+8a*—has been shown to play a key role in promoting neuronal differentiation in the developing brain. We previously determined that *LSD1+8a* transcripts were detected in an aggressive subtype of prostate cancer harboring a neuronal program—neuroendocrine prostate cancer (NEPC)—but not in prostate adenocarcinomas harboring a glandular program. However, the number of samples examined was limited.

Methods: Using a large collection of prostate cancer patient cell lines and patient-derived xenografts (PDXs), we measured LSD1+8a using quantitative polymerase chain reaction (qPCR), RNA *in situ* hybridization (RNA-ISH), and protein detection methods. We then validated our findings using an independent cohort of patient tumor samples.

Results: LSD1+8a mRNA expression was detected in every NEPC cell line and PDX examined by qPCR and RNA-ISH but in none of the prostate adenocarcinomas. We validated the RNA-ISH results in patient tumors, confirming that *LSD1+8a* was expressed in all NEPC tumors but in none of the adenocarcinomas. Finally, we generated a rabbit monoclonal antibody specific to LSD1+8a protein and confirmed its specificity using normal neuronal tissue samples. However, LSD1+8a protein was not detectable in NEPC tumors—likely due to the substantially lower levels of *LSD1+8a* mRNA in NEPC tumors vs. normal neuronal tissues.

Conclusions: Measuring *LSD1*+8a mRNA is a sensitive and specific method for the diagnosis of NEPC, which is often challenging.

Introduction

Prostate cancer is the second leading cause of cancer-related death in men in the United States, with 35,250 deaths predicted for 2024 [1]. Prostate adenocarcinoma is the predominant form of prostate cancer at diagnosis (99 %). However, other subtypes—namely neuroendocrine

Abbreviations: AR, Androgen receptor; ARPI, AR pathway inhibitor; LSD1, Lysine-specific demethylase 1; LSD1+8a, Lysine-specific demethylase 1 8a splice variant; NEPC, Neuroendocrine prostate cancer; PDX, Patient-derived xenograft; RNA-ISH, RNA *in situ* hybridization.

* Corresponding author at: 7312 Rogel Cancer Center, SPC 5948, 1500 East Medical Center Drive, Ann Arbor, MI 48109, USA.
E-mail address: jalumkal@med.umich.edu (J.J. Alumkal).

[1] Contributed equally.

https://doi.org/10.1016/j.neo.2025.101151
Received 7 January 2025; Accepted 6 March 2025

prostate cancer expressing a neuronal program—are sometimes identified (1 %) at diagnosis [2]. Androgen receptor (AR) blockade is the principal treatment for metastatic prostate adenocarcinoma. One increasingly recognized form of resistance to AR blockade is lineage plasticity, or differentiation change, and this form of resistance has increased in the era of newer, more potent AR pathway inhibitors (ARPIs) [3,4]. Treatment-emergent NEPC is one of the most common and virulent examples of lineage plasticity after AR pathway inhibition, occurring in ~15 % of patients who have been treated with ARPIs [5]. NEPC is aggressive, and there are limited treatment options [4,5]. However, the diagnosis of NEPC can be challenging and is based on both morphologic and molecular features [6,7]. Identifying additional biomarkers could help diagnose NEPC with more accuracy.

Lysine-specific demethylase 1 (LSD1) is a histone demethylase and important regulator of gene expression in multiple cancers [8–12]. LSD1 has been shown to promote AR-independent survival of castrate-resistant prostate cancers that grow well despite AR blockade [8]. Our recent work showed that LSD1 also promotes growth and survival of NEPC tumor models [9]. Importantly, a neuronal-specific isoform of *LSD1—LSD1+8a*—that includes a cryptic exon 8 was identified and shown to play an important role during brain development by regulating neuronal differentiation [13,14]. *LSD1+8a* has also been shown to promote neuronal differentiation in small cell lung cancer, which harbors many similarities with NEPC, prompting us to examine *LSD1+8a* in NEPC [15].

Previously, we measured *LSD1+8a* expression with quantitative PCR (qPCR) in a limited collection of samples and determined that *LSD1+8a* transcripts were expressed in NEPC patient-derived xenografts (PDXs) and patient tumors—but not in adenocarcinoma patient samples and PDX [16]. We also found that the splicing factors SRRM3 and SRRM4 were responsible for LSD1+8a splicing in NEPC [16,17]. However, because of the limited number of samples tested, it was not clear whether LSD1+8a was a sensitive and specific biomarker to detect NEPC. Furthermore, because antibodies to measure LSD1+8a protein expression were lacking, it was not clear if LSD1+8a protein was expressed in these tumors in sufficient quantities to contribute to neuronal differentiation.

Herein, we examined LSD1+8a expression in a large collection of prostate cancer patient tumors using RNA and protein-based detection methods. Using qPCR, *LSD1+8a* transcripts were detected exclusively in NEPC tumors, and we confirmed our findings using RNA *in situ* hybridization (RNA-ISH). However, while LSD1+8a protein expression was detectable in normal neuronal tissues, we failed to detect LSD1+8a protein in any of the NEPC tumors examined—likely due to the substantially lower levels of *LSD1+8a* mRNA in NEPC tumors vs. normal neuronal tissues. In summary, measuring *LSD1+8a* mRNA may aid in the diagnosis of NEPC due to the sensitivity and specificity of this biomarker.

Results

LSD1+8a transcript is expressed only in NEPC

We previously detected *LSD1+8a* transcript expression in a limited number of NEPC PDXs and metastatic biopsies using qPCR [16]. Building on this result, we measured *LSD1+8a* transcript abundance using qPCR in a panel of prostate cancer cell lines, including adenocarcinomas, models reprogrammed from adenocarcinomas but that do not represent canonical NEPC [18,19], and NEPC tumors. We used *LSD1+8a*-overexpressing LNCaP adenocarcinoma cells as a positive control (Fig. 1A). Low, but detectable, levels of *LSD1+8a* transcript were observed only in NEPC cell lines but not in adenocarcinoma or reprogrammed prostate cancer cell line models (Fig. 1A). Of note, the levels of endogenous *LSD1+8a* expression in NEPC cell lines were several logs lower than that of the ectopically-expressing *LSD1+8a* positive control cell line.

Next, we tested a panel of adenocarcinoma and NEPC PDX models and patient tumors. The *LSD1+8a* sequence is conserved between mouse and human (Supplementary Fig. S1A, B) and is expressed in human and mouse brain [14]. Therefore, we used mouse and human brain RNA as positive controls. Importantly, the levels of *LSD1+8a* in the normal neuronal tissues were comparable to the expression levels in the LNCaP-*LSD1+8a* cells we generated (Fig. 1A). *LSD1+8a* transcripts were present in all the NEPC PDXs and patient tumors examined—though the expression levels were several logs lower than the normal neuronal tissues (Fig. 1B). Conversely, *LSD1+8a* was not expressed in any of the adenocarcinoma PDXs and patient tumors examined (Fig. 1B).

RNA in situ hybridization assays detect LSD1+8a specifically in NEPC tumors

Having determined that *LSD1+8a* transcripts are expressed specifically in NEPC patient models and tumors by qPCR, we sought to test a method to measure *LSD1+8a* transcripts more easily that could be used clinically. Therefore, we developed an RNA *in situ* hybridization probe to specifically detect *LSD1+8a* transcripts (Supplementary Table-1). To validate the probe, we used cell blocks prepared with LNCaP cells overexpressing expressing empty vector or *LSD1+8a*. We also used a

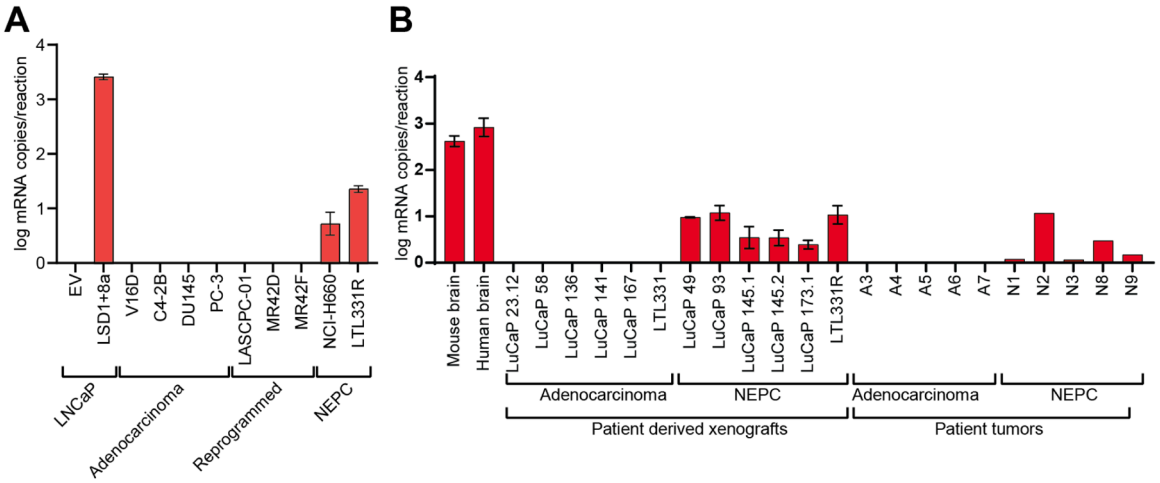

Fig. 1. *LSD1+8a* transcripts are expressed only in NEPC. (A) *LSD1+8a* transcripts were measured in prostate cancer cell lines by qPCR. Empty vector (EV) LNCaP cells served as a negative control. *LSD1+8a-over*expressing LNCaP cells served as a positive control. (B) *LSD1+8a* transcripts were measured in PDXs and patient samples by qPCR. Normal mouse and human brain samples served as positive controls.

probe for the bacterial transcript *DAPB* as a negative control and a probe for the human transcript *PPIB* as a positive control for RNA integrity. RNA-ISH showed that *LSD1+8a* was detectable in *LSD1+8a*-overexpressing LNCaP cells but not empty vector cells, demonstrating the specificity of the probes for detecting *LSD1+8a* (Fig. 2A, B). *DAPB* was not detectable while *PPIB* was detectable across all the samples, demonstrating the sensitivity and specificity of the assay (Supplementary Fig. S2A).

We next tested the RNA-ISH probes using PDX samples. Importantly, the NEPC PDXs express much lower quantities of *LSD1+8a* transcript than the *LSD1+8a*-overexpressing LNCaP cells or normal mouse or human neuronal tissues (Fig. 1A, B). Matching the qPCR results, RNA-ISH only identified *LSD1+8a* expression in NEPC PDXs but not in adenocarcinoma PDXs (Fig. 2C, D, Supplementary Table-2). Of note, RNA-ISH showed a heterogeneous expression pattern for *LSD1+8a* transcripts with only certain tumor cells expressing the transcript (Fig. 2D). We confirmed the RNA quality of these samples using the positive control human *PPIB* probe and set a threshold of 75 based on the distribution of PPIB scores in the PDX samples we tested (Supplementary Fig. 2B, Supplementary Table-2).

Finally, we sought to validate our *LSD1+8a* RNA-ISH results using archived prostate cancer patient tumors. These included 25 NEPC and 134 adenocarcinoma samples. Importantly, many of these samples were greater than five years old, making them susceptible to RNA degradation. Therefore, we used the *PPIB* probe to confirm the RNA quality of all samples (Supplementary Fig. 2C, Supplementary Table-3). Based on the threshold set for PPIB based on the PDX samples, eighty-two adenocarcinoma samples and ten NEPC samples passed *PPIB* quality control, indicating good RNA quality (Fig. 3A, Supplementary Fig. 2D, Supplementary Table-3). Of the samples with good RNA quality, *LSD1+8a*

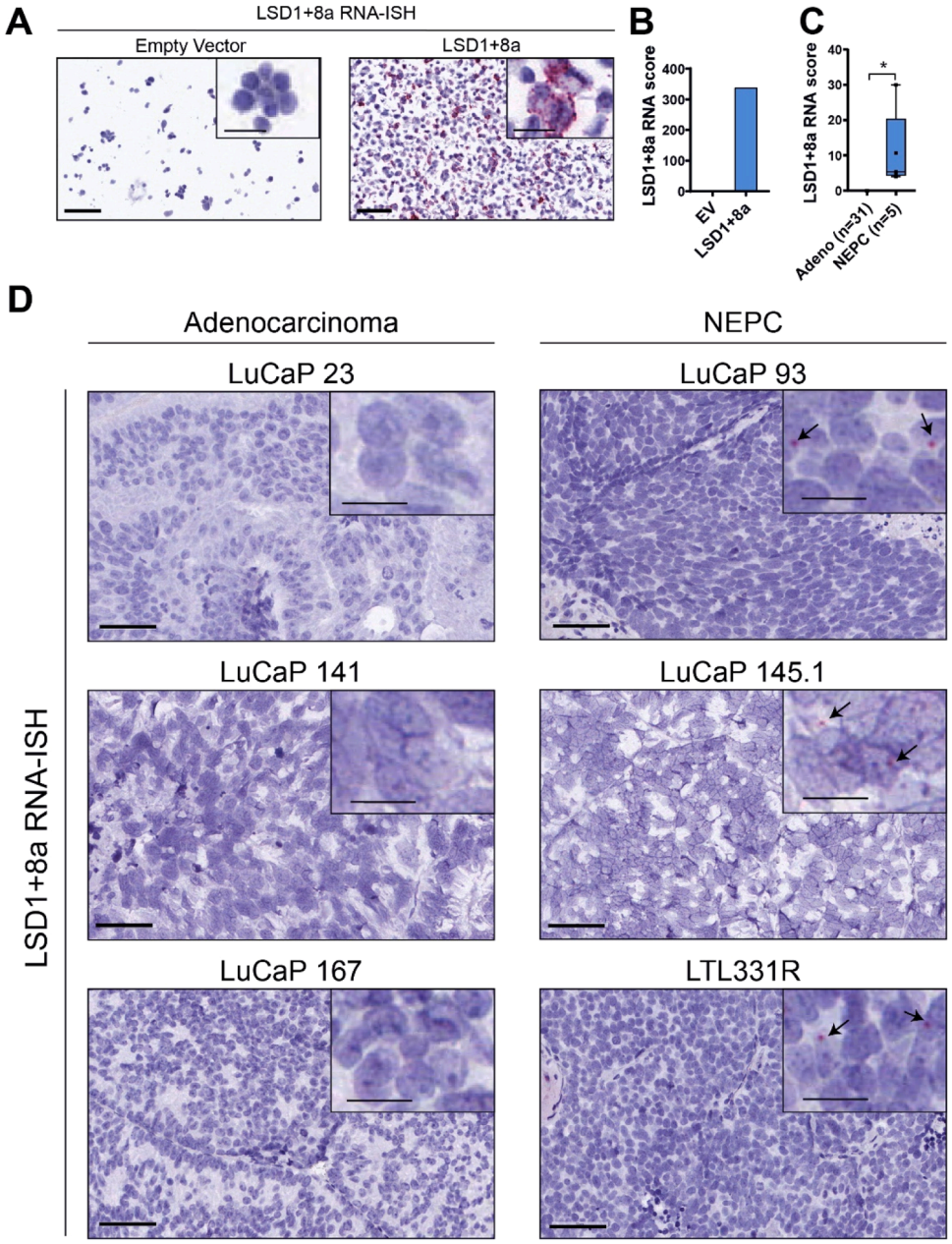

Fig. 2. *LSD1+8a* transcripts are detected by RNA-ISH in NEPC PDXs. (A) *LSD1+8a* transcripts are detectable by RNA-ISH in *LSD1+8a*-overexpressing cells but not in empty vector cells. (B and C) RNA-ISH score of *LSD1+8a* in (B) cell lines and (C) PDXs. (D) *LSD1+8a* transcripts are detectable by RNA-ISH in NEPC PDXs but not adenocarcinoma PDXs ($N = 36$). Scalebar represents 60μm, inset is 15μm.

A

Phenotype	Samples that passed QC	*LSD1+8a* transcript ISH detected
Adenocarcinoma	82	0
NEPC	10	10

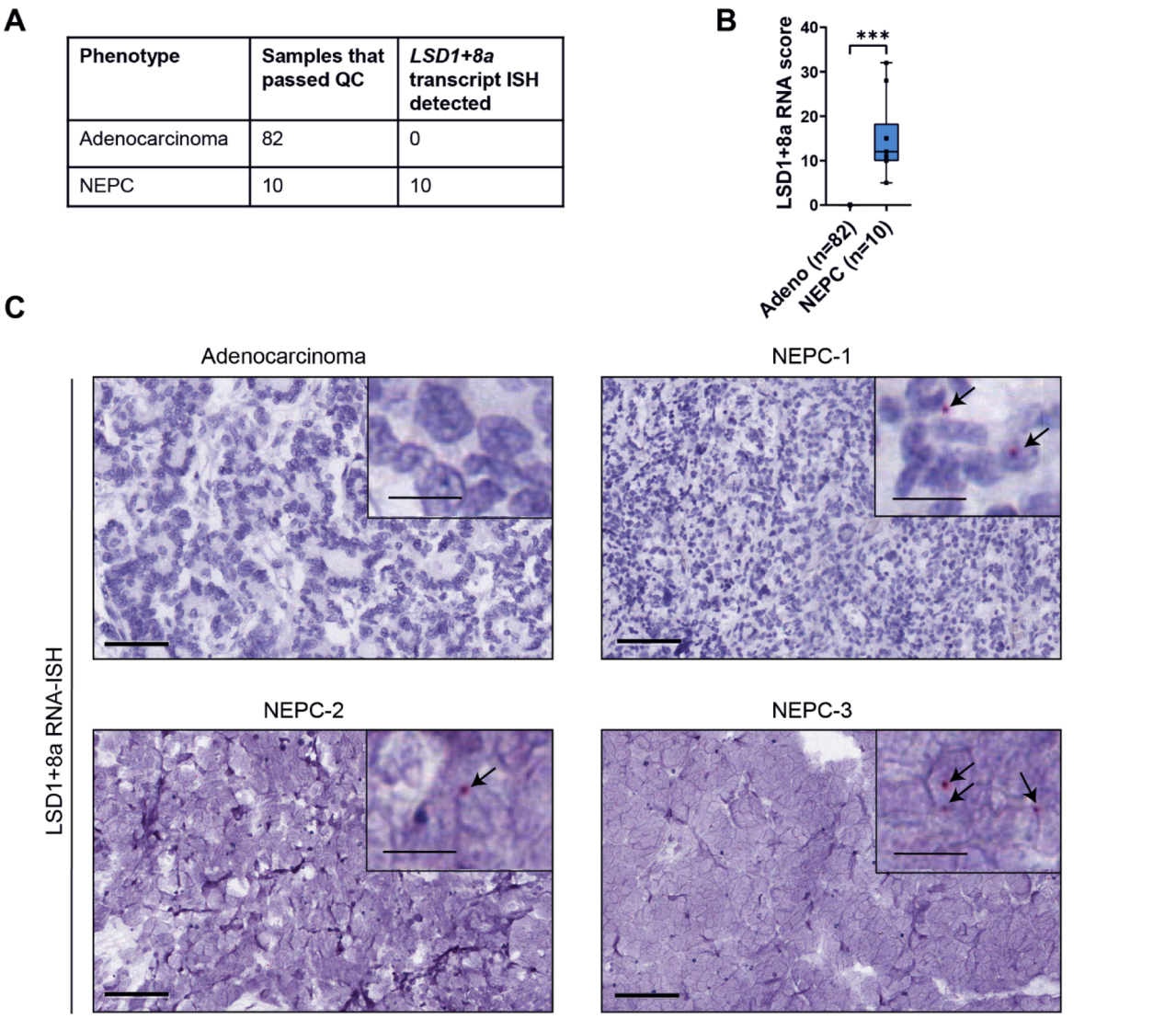

Fig. 3. *LSD1+8a* transcripts are detected by RNA-ISH in NEPC tumors. (A) Table indicating number of samples that passed RNA integrity metrics in which *LSD1+8a* was detectable by RNA-ISH. (B) RNA-ISH scores of *LSD1+8a* in patient tumors. (C) Representative images showing detectable *LSD1+8a* transcripts by RNA-ISH in NEPC patient tumors but not in prostate adenocarcinoma patient tumors. Scalebar represents 60μm, inset is 15μm.

transcripts were detected by RNA-ISH with a heterogeneous pattern of tumor cell expression in all 10 NEPC samples but in none of the 82 adenocarcinoma samples (Fig. 3B, C), demonstrating 100 % specificity and sensitivity of *LSD1+8a* RNA-ISH for identifying NEPC tumors.

LSD1+8a protein levels are not detectable in LSD1+8a mRNA-expressing NEPC PDXs and patient tumors

As previously mentioned, *LSD1+8a* mRNA expression was several logs lower in NEPC cell lines, PDX, and patient tumors by qPCR vs. normal mouse or human neuronal tissues. Nevertheless, we sought to determine whether LSD1+8a protein expression was detectable in NEPC tissues. Suitable antibodies to measure LSD1+8a were not available. To address that deficit, we generated a rabbit monoclonal antibody against LSD1+8a.

To determine the specificity and sensitivity of the antibody, we tested the antibody using LNCaP FLAG-*LSD1+8a* or empty vector cells. We confirmed that FLAG expression was only detectable in the *LSD1+8a* transfected cells by Western blotting (Supplementary Fig. 3 A). We next tested the specificity of our LSD1+8a antibody at three different dilutions in by Western blot analysis. Western blotting indicated that the LSD1+8a antibody showed a strong, specific signal at 1:10,000 dilution (Fig. 4A).

We next sought to measure endogenous LSD1+8a protein expression in NEPC patient samples and model systems, including those we previously determined to express *LSD1+8a* transcripts (Fig. 1) [16]. We used *LSD1+8a*-overexpressing LNCaP cells as a positive control. While LSD1+8a was detectable in LNCaP-*LSD1+8a* cells, we did not detect LSD1+8a in any other cell line, including the two NEPC cell lines NCI-H660 and LTL331R that expressed lower but detectable levels of *LSD1+8a* transcript vs. *LSD1+8a*-overexpressing LNCaP (Fig. 1A, Supplementary Fig. 3B). Next, we measured LSD1+8a protein levels in adenocarcinoma and NEPC PDXs by Western blot. We included human brain as a positive control for endogenous LSD1+8a protein expression. Even at higher exposures, where LSD1+8a protein was detectable in human brain, all the PDX samples were negative for LSD1+8a protein by Western blotting (Supplementary Fig. 3C). Because *LSD1+8a* transcripts are expressed at much lower level vs. normal control tissues and because of the heterogenous mRNA expression pattern in NEPC samples, it is possible that the levels of LSD1+8a protein are too low to be detected by Western blotting.

We next determined whether LSD1+8a was detectable in NEPC

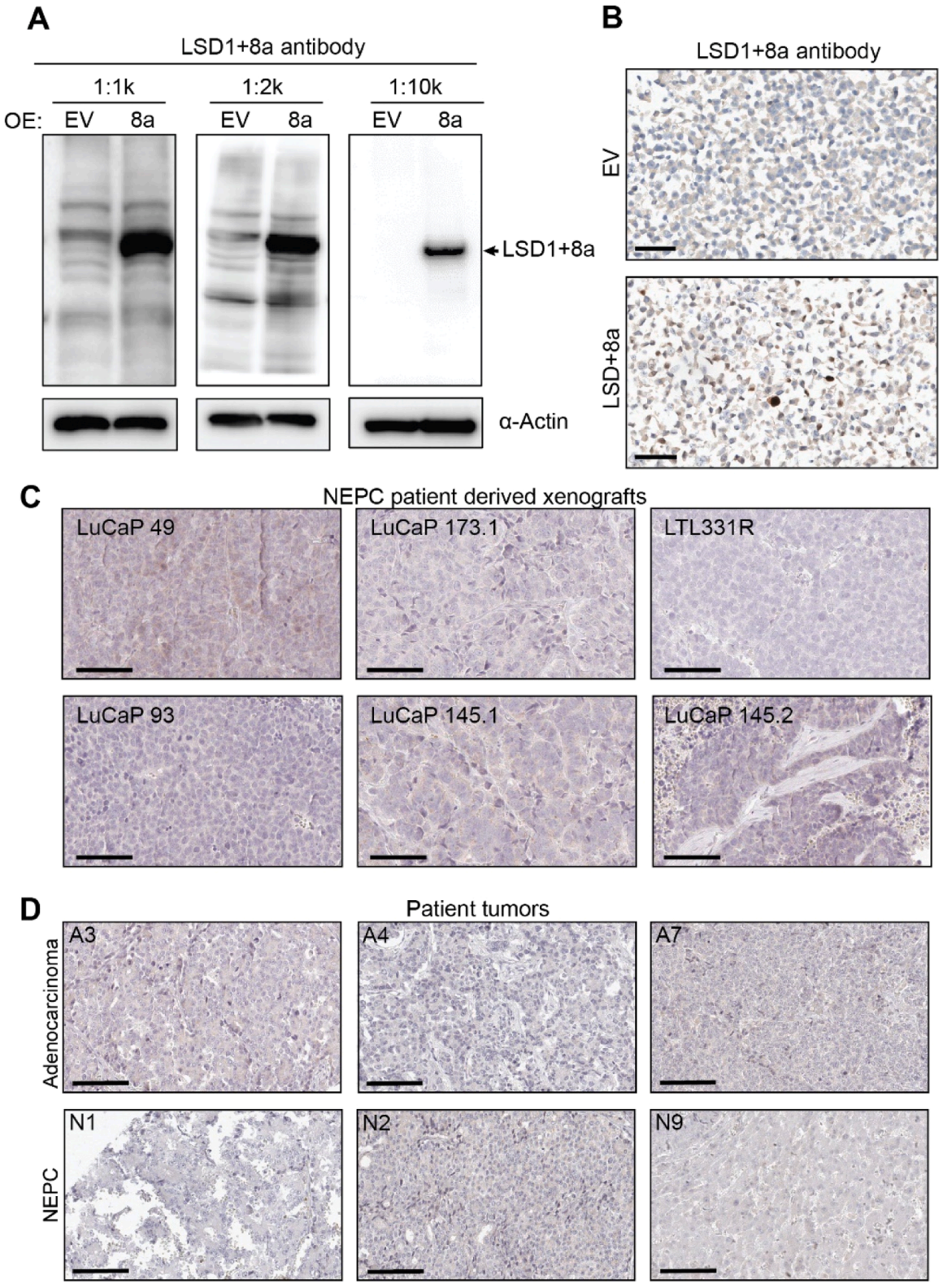

Fig. 4. LSD1+8a protein is undetectable in transcript-positive NEPC PDXs and tumors by IHC. (A) Western blotting confirms LSD1+8a antibody detects LSD1+8a protein in *LSD1+8a*-overexpressing (OE) cells but not empty vector (EV) cells. A 1:10,000 dilution provided the most specific results. (B) IHC analysis indicates LSD1+8a antibody detects LSD1+8a protein in *LSD1+8a*-overexpressing cells (LSD1+8a) but not in EV cells. (C and D) Representative images from IHC staining shows absent LSD1+8a protein expression in (C) NEPC PDX samples and (D) patient tumor samples. Scalebar represents 80μm.

samples using immunohistochemistry (IHC). We used cell blocks from LNCaP cells overexpressing empty vector or *LSD1+8a* as controls. Analysis of IHC data showed LSD1+8a nuclear staining in *LSD1+8a*-overexpressing cells but not in empty vector cells (Fig. 4B). We then measured endogenous LSD1+8a protein expression by IHC in NEPC PDXs and patient samples using a tissue microarray (TMA) of 38 PDX samples, including six NEPC PDXs, and another TMA of 99 prostate cancer patient samples, including 21 NEPC samples. These TMAs included five NEPC PDXs and five NEPC patient tumor samples from which we had observed detectable levels of *LSD1+8a* transcripts (Fig. 1B). However, LSD1+8a protein was not detectable in any of the PDXs (Fig. 4C, Supplementary Table-4) or patient samples (Fig. 4D, Supplementary Table-3) despite the antibody detecting endogenous LSD1+8a protein expression in normal human brain samples (Supplementary Fig. 3D), possibly due to the much lower *LSD1+8a* mRNA expression in human NEPC tumors.

Discussion

NEPC is the most virulent subtype of prostate cancer, and its frequency appears to be increasing due to more widespread use of potent ARPIs [5]. However, the clinical diagnosis of NEPC can sometimes be challenging, especially for treatment-emergent forms of the disease that do not always have the classic morphological characteristics [2,5,7].

LSD1+8a is a neuronal isoform of *LSD1* that has been shown to play a role in neuronal differentiation of neural tissues and in small cell lung cancer [13–15]. Because we previously determined that *LSD1+8a* was expressed at the mRNA level in a small collection of NEPC samples [16], our goal was to determine the specificity and sensitivity of mRNA-based and protein-based measurements of LSD1.

RNA-based biomarkers in prostate cancer are available for adenocarcinoma to detect androgen receptor (AR) splice variants and AR targets [20–22]. Our group has previously determined that RNA-ISH detection of the long non-coding RNA SChLAP1 in prostate adenocarcinoma tumors is associated with prostate cancer lethality [23]. However, there are no RNA biomarkers specific to NEPC in routine clinical use. The high sensitivity of RNA-ISH is advantageous to detect low levels of transcripts whose protein products may not be detectable by IHC-based methods; furthermore, RNA-ISH is easier to perform in a clinical lab than qPCR [24,25]. Increased sensitivity and the ability to multiplex probes for multiple transcripts makes RNA-ISH quite attractive for clinical use in determining disease states [25]. Finally, RNA-ISH allows spatial detection of the biomarker of interest, allowing for a clearer pattern of gene expression than qPCR.

Using cell lines and PDXs, we confirmed that *LSD1+8a* mRNA expression was only detectable by qPCR in NEPC samples, matching our prior results [16]. Importantly, cell lines representing reprogrammed prostate cancer cells that do not harbor a canonical NEPC program failed to express *LSD1+8a*, further demonstrating the specificity of this marker for NEPC.

Validating our results from cell lines and PDXs, RNA-ISH detected *LSD1+8a* in all NEPC patient tumors examined but none of the adenocarcinoma tumors, suggesting *LSD1+8a* transcript may be a sensitive and specific biomarker to detect NEPC.

Unlike qPCR and RNA-ISH, we failed to detect LSD1+8a protein in any NEPC sample using an LSD1+8a antibody that we confirmed to be sensitive and specific. Like the pattern we observed for *LSD1+8a*, previous studies have shown a discrepancy between mRNA expression of genes and their protein levels [26,27]. There are several explanations for the discrepancy between detectable *LSD1* mRNA and undetectable protein. First, the levels of *LSD1+8a* transcript are 10 to 100-fold lower in NEPC samples vs. our positive control *LSD1+8a*-expressing tissues (i.e., mouse and human brain and *LSD1+8a* overexpressing LNCaP cells). Thus, the much lower mRNA levels of *LSD1+8a* in these tissues may lead to a limited, undetectable pool of LSD1+8a protein using the assays we performed. Potentially utilizing more sensitive approaches such as high-resolution microscopy or mass spectrometry might enable us to detect low quantities of LSD1+8a protein that are not detectable by Western blotting or IHC [28,29]. Other possibilities that may explain why we failed to detect LSD1+8a protein despite detectable mRNA include dissociation between mRNA and protein levels. A global proteomic based study found that mRNA levels explain only about 40 % of the variability in protein levels, whereas a model based on translational mechanisms was a better predictor of protein level changes (~60 %) [30,31]. As observed for IL-1 beta, translational efficiency can determine the level of protein expressed and may result in detectable mRNA but lower or undetectable protein [32]. More studies are warranted to explore if there are translational impediments to LSD+8a protein expression.

Like all RNA-based detection methods, RNA-ISH relies heavily on the integrity of the RNA in tissue samples. Our results using a marker of RNA integrity (*PPIB* probe), suggest that RNA degradation occurred in many archived patient tumor samples we examined (88 out of 175), which may have interfered with our ability to detect *LSD1+8a* by RNA-ISH in some samples—especially since *LSD1+8a* levels are low to begin with. Thus, it may be important to measure *LSD1+8a* on recently obtained tumor specimens that have not been undergone RNA degradation, rather than previously archived samples that are many years old.

In summary, our results suggest that *LSD1+8a* mRNA was exclusively detected in NEPC samples but not prostate adenocarcinoma samples. Thus, *LSD1+8a* appears to be a sensitive and specific biomarker for NEPC. RNA-ISH that is routinely performed clinically—and perhaps protein detection methods with better antibodies in the future—may aid in the diagnosis of NEPC.

Materials and methods

Cell lines

LASCPC-01, MR42D, and LNCaP cells were cultured as described previously [9,18,19]. NCI-H660 cells (CRL-5813) were purchased from ATCC and cultured according to their recommendation. LNCaP cells overexpressing *LSD1+8a* were described previously [16]. All cell lines were validated with STR DNA fingerprinting (Genetica) and regularly tested for Mycoplasma contamination using the MycoAlert Mycoplasma Detection Kit (Lonza cat# LT07-318).

Antibody development

LSD1+8a antibodies were generated and developed by RevMAb Biosciences, USA using a standard rabbit immunization protocol and its rabbit monoclonal antibody development technology platform. Briefly, New Zealand White (NZW) rabbits were immunized with a LSD1+8a peptide, its amino acid sequence corresponding to human LSD1+8a protein sequence, conjugated to keyhole limpet hemocyanin (KLH) carrier protein. After 4 boosts, blood (30 ml/rabbit) was sampled for memory B cell isolation, using the LSD1+8a peptide. After culturing the B cells for 8 days, supernatants were tested for antibody specificity to the peptide by ELISA and screened by WB using cell lysates from human *LSD1+8a* overexpressing cells and by IHC using paraffin embedded cell blocks. For B cell clones identified by WB and IHC, their antibody DNA fragments for the entire L chain and the variable region of H chain (VH) of rabbit IgG were amplified by PCR with rabbit IgG H and L chain primers, and then inserted into mammalian expression vectors with or without built-in constant region of rabbit antibody H chain. The resulted plasmids were used to express full-length recombinant antibodies in HEK293 suspension cells (Thermo Fisher Scientific cat# R79007). The recombinant antibodies were confirmed by WB and IHC for their detection of LSD1+8a in overexpressed cells and then further tested with human and mouse brain tissues. Based on WB and IHC analysis, LSD1+8a antibody (Clone RM523) (RevMAb Biosciences cat# 31-1415-00; RRID - AB_3674472) specifically detects LSD1+8a protein.

Western blotting

Western blotting experiments were performed by running homogenized PDX or cell lysates on NuPAGE 4-12 % Bis-Tris protein gels (Thermo Fisher Scientific cat# NP0335BOX) and transferring them onto PVDF membranes as described previously [9]. Blots were probed with indicated primary antibodies (LSD1 – Cell Signaling Technologies cat#2139S; Flag – Sigma Aldrich cat# F1804, Actin – Sigma Aldrich cat# A5441) and HRP-conjugated secondary antibodies (Rockland cat#611-703-127). West dura extended duration substrate chemiluminescence kit (Thermo Fisher Scientific cat#34075) was used to develop signal and imaged using a Chemidoc MP imaging system (Bio-Rad).

RNA preparation and RT-qPCR

RNA was extracted from cells, PDXs, or tissues using the RNeasy Plus Mini Kit (Qiagen cat# 74034) according to the manufacturer's protocol. After RNA extraction, 1 μg RNA was reverse-transcribed into cDNA using the High-Capacity cDNA Reverse Transcription kit (Life Technologies cat# 4368814) with random hexamer primers. RT-qPCR was performed using PowerUp™ SYBR™ Green Master Mix (Thermo Fisher Scientific cat# A25742) in a Quantstudio 3 thermocycler (Life Technologies) with the following program: 50 °C for 2 min, 95°C for 10 min, and 40 cycles of 95°C for 15 s dissociation, 60°C for 1 min annealing/extension/read. Data were analyzed with Design and Analysis Software version 1.5.2 (Life Technologies). Standard curve was generated as described previously [16].

Immunohistochemistry

Immunohistochemistry was performed on 5μm formalin-fixed, paraffin-embedded tissue sections. Metastatic CRPC specimens were collected from patients who died of CRPC and signed written informed consent for a rapid autopsy under the aegis of the Prostate Cancer Donor Program at the University of Washington (IRB protocol # 2341). The Ventana Discovery staining platform with ULTRA Cell Conditioning (ULTRA CC2) solution (Ventana cat# 950-223) was used for antigen retrieval. Anti-LSD1+8a antibodies were used at 1:1000. Immune complexes were developed using the Discovery ChromoMap DAB (diaminobenzidine tetrahydrochloride) Detection Kit (Ventana cat# 760-159).

RNA in-situ hybridization

RNA-ISH was performed on 5μM FFPE tissue sections using the BaseScope Detection Reagent kit v2- RED (Advanced Cell Diagnostics, Newark, CA) and a target probe against *BA-Hs-KDM1A-tv1-E9E*10 (Homo sapiens lysine demethylase 1A (KDM1A) transcript variant 1 mRNA). The RNA quality of the samples was assessed using *BA-Hs-PPIB-1zz* (Homo sapiens peptidylprolyl isomerase B (cyclophilin B) (PPIB) positive control probe) and *DapB-1ZZ* – BaseScope Negative Control Probe. RNA-ISH signals in tumor cells were studied by the study pathologist Rahul Mannan. The RNA-ISH data and quantitative scoring in the present study cohort *for BA-Hs-KDM1A-tv1-E9E10* were conducted as per manufacturer recommendations and as described previously [33]. The number of red punctate dots (each dot corresponding to a single RNA molecule) and clusters per cell were counted and recorded. The details of reagents are provided in Supplementary Table-1.

Sequence alignment

Nucleotide and mRNA sequences for the human and mouse *KDM1A* gene were retrieved from NCBI reference sequence database. CLUSTALW tool (https://www.genome.jp/tools-bin/clustalw; accessed on 2024-03-01) was used for performing clustal 2.1 multiple sequence alignment using default settings by selecting sequence type as DNA (for nucleotide sequences) or PROTEIN (for amino acid sequences). Alignment around the *LSD1+8a* insert is represented in Supplementary Figure-1.

Statistics

GraphPad Prism version 10.0.1 was used for statistical analysis and plotting graphs. For statistical analysis, unpaired Student's t-test was performed, and a $p < 0.05$ is considered significant.

Funding and Acknowledgements

We would like to thank the patients who generously donated tissue under University of Washington TAN program that made this research possible. The characterization and maintenance of the LuCaP PDX models was supported by the Pacific Northwest Prostate Cancer SPORE (P50 CA97186), the PO1 NIH grant (PO1 CA163227) and the Institute of Prostate Cancer Research. This work was supported by: NCI R01 CA251245, R01 CA282005, R01 CA234715; the Pacific Northwest Prostate Cancer SPORE/NCI P50 CA097186; the Michigan Prostate SPORE/NCI P50 CA186786 and P50 CA186786-07S1; University of Michigan Rogel Innovation Award P30 046592; University of Michigan Rogel Scholar Award; Department of Defense (DOD) Idea Award W81XWH-20-1-0405; Joint Institute for Cancer Research Award, and Smith Family Fellowship.

CRediT authorship contribution statement

Anbarasu Kumaraswamy: Conceptualization, Data curation, Formal analysis, Investigation, Project administration, Visualization, Writing – original draft, Writing – review & editing. **Rahul Mannan:** Data curation, Formal analysis, Investigation, Methodology, Visualization, Writing – original draft, Writing – review & editing. **Olivia A. Swaim:** Data curation, Formal analysis, Investigation, Writing – original draft, Writing – review & editing. **Eva Rodansky:** Formal analysis, Investigation. **Xiao-Ming Wang:** Formal analysis. **Aaron Udager:** Resources. **Rohit Mehra:** Resources, Writing – review & editing. **Hui Li:** Resources. **Colm Morrissey:** Resources, Writing – review & editing. **Eva Corey:** Resources, Writing – review & editing. **Michael C. Haffner:** Resources, Writing – review & editing. **Peter S. Nelson:** Resources, Writing – review & editing. **Arul M. Chinnaiyan:** Resources. **Joel A. Yates:** Formal analysis, Visualization, Writing – original draft. **Joshi J. Alumkal:** Conceptualization, Formal analysis, Funding acquisition, Investigation, Project administration, Resources, Supervision, Writing – original draft, Writing – review & editing.

Declaration of competing interest

The authors declare the following financial interests/personal relationships which may be considered as potential competing interests:

Dr. Alumkal has received consulting fees from Fortis Therapeutics and ORIC Pharmaceuticals, and research support to his institution from Beactica and Zenith Epigenetics outside of the submitted work. His institution has also received research support from a National Comprehensive Cancer Network (NCCN)/Astellas Pharma Global Development, Inc./Pfizer, Inc. research award outside of the submitted work. EC served as a paid consultant to DotQuant and received institutional sponsored research funding unrelated to this work from AstraZeneca, AbbVie, Gilead, Sanofi, Zenith Epigenetics, Bayer Pharmaceuticals, Forma Therapeutics, Genentech, GSK, Janssen Research, Kronos Bio, Foghorn Therapeutics, and MacroGenics. P.S.N. has served as a paid advisor for Bristol Myers Squibb, Pfizer, Genentech, AstraZeneca, and Janssen and received research support from Janssen.

Supplementary materials

Supplementary material associated with this article can be found, in the online version, at doi:10.1016/j.neo.2025.101151.

References

[1] R.L. Siegel, A.N. Giaquinto, A. Jemal, Cancer statistics, 2024, CA Cancer J. Clin. 74 (1) (2024) 12–49, https://doi.org/10.3322/caac.21820. Jan-Feb.

[2] A.D. Grigore, E. Ben-Jacob, Farach-Carson MC, Prostate cancer and neuroendocrine differentiation: more neuronal, less endocrine? Front. Oncol. 5 (2015) 37, https://doi.org/10.3389/fonc.2015.00037.

[3] W.K. Storck, A.M. May, T.C. Westbrook, et al., The role of epigenetic change in therapy-induced neuroendocrine prostate cancer lineage plasticity, Front. Endocrinol. (Lausanne) 13 (2022) 926585, https://doi.org/10.3389/fendo.2022.926585.

[4] H. Beltran, D. Prandi, J.M. Mosquera, et al., Divergent clonal evolution of castration-resistant neuroendocrine prostate cancer, Nat. Med. 22 (3) (2016) 298–305, https://doi.org/10.1038/nm.4045. Mar.

[5] R. Aggarwal, J. Huang, J.J. Alumkal, et al., Clinical and genomic characterization of treatment-emergent small-cell neuroendocrine prostate cancer: a multi-institutional prospective study, J. Clin. Oncol. 36 (24) (2018) 2492–2503, https://doi.org/10.1200/JCO.2017.77.6880. Aug 20.

[6] C. Zhang, J. Qian, Y. Wu, et al., Identification of novel diagnosis biomarkers for therapy-related neuroendocrine prostate cancer, Pathol. Oncol. Res. 27 (2021) 1609968, https://doi.org/10.3389/pore.2021.1609968.

[7] M.C. Haffner, M.J. Morris, C.C. Ding, et al., Framework for the pathology workup of metastatic castration-resistant prostate cancer biopsies, Clin. Cancer Res. (2024), https://doi.org/10.1158/1078-0432.CCR-24-2061. Nov 26.

[8] A. Sehrawat, L. Gao, Y. Wang, et al., LSD1 activates a lethal prostate cancer gene network independently of its demethylase function, Proc. Natl. Acad. Sci. U S A 115 (18) (2018) E4179–E4188, https://doi.org/10.1073/pnas.1719168115. May 1.

[9] A. Kumaraswamy, Z. Duan, D. Flores, et al., LSD1 promotes prostate cancer reprogramming by repressing TP53 signaling independently of its demethylase function, JCI. Insight. 8 (15) (2023), https://doi.org/10.1172/jci.insight.167440. Aug 8.

[10] D.E. Park, J. Cheng, J.P. McGrath, et al., Merkel cell polyomavirus activates LSD1-mediated blockade of non-canonical BAF to regulate transformation and tumorigenesis, Nat. Cell Biol. 22 (5) (2020) 603–615, https://doi.org/10.1038/s41556-020-0503-2. May.

[11] S. Egolf, Y. Aubert, M. Doepner, et al., LSD1 Inhibition promotes epithelial differentiation through derepression of fate-determining transcription factors, Cell Rep. 28 (8) (2019) 1981–1992, https://doi.org/10.1016/j.celrep.2019.07.058. Aug 20e7.

[12] A. Augert, E. Eastwood, A.H. Ibrahim, et al., Targeting NOTCH activation in small cell lung cancer through LSD1 inhibition, Sci. Signal. 12 (567) (2019), https://doi.org/10.1126/scisignal.aau2922. Feb 5.

[13] B. Laurent, L. Ruitu, J. Murn, et al., A specific LSD1/KDM1A isoform regulates neuronal differentiation through H3K9 demethylation, Mol. Cell 57 (6) (2015) 957–970, https://doi.org/10.1016/j.molcel.2015.01.010. Mar 19.

[14] C. Zibetti, A. Adamo, C. Binda, et al., Alternative splicing of the histone demethylase LSD1/KDM1 contributes to the modulation of neurite morphogenesis in the mammalian nervous system, J. Neurosci. 30 (7) (2010) 2521–2532, https://doi.org/10.1523/JNEUROSCI.5500-09.2010. Feb 17.

[15] T. Jotatsu, S. Yagishita, K. Tajima, et al., LSD1/KDM1 isoform LSD1+8a contributes to neural differentiation in small cell lung cancer, Biochem. Biophys. Rep. 9 (2017) 86–94, https://doi.org/10.1016/j.bbrep.2016.11.015. Mar.

[16] D.J. Coleman, D.A. Sampson, A. Sehrawat, et al., Alternative splicing of LSD1+8a in neuroendocrine prostate cancer is mediated by SRRM4, Neoplasia 22 (6) (2020) 253–262, https://doi.org/10.1016/j.neo.2020.04.002. Jun.

[17] M.P. Labrecque, L.G. Brown, I.M. Coleman, et al., RNA splicing factors SRRM3 and SRRM4 distinguish molecular phenotypes of castration-resistant neuroendocrine prostate cancer, Cancer Res. 81 (18) (2021) 4736–4750, https://doi.org/10.1158/0008-5472.CAN-21-0307. Sep 15.

[18] J.L. Bishop, D. Thaper, S. Vahid, et al., The master neural transcription factor BRN2 is an androgen receptor-suppressed driver of neuroendocrine differentiation in prostate cancer, Cancer Discov. 7 (1) (2017) 54–71, https://doi.org/10.1158/2159-8290.CD-15-1263. Jan.

[19] J.K. Lee, J.W. Phillips, B.A. Smith, et al., N-Myc drives neuroendocrine prostate cancer initiated from Human prostate epithelial cells, Cancer Cell 29 (4) (2016) 536–547, https://doi.org/10.1016/j.ccell.2016.03.001. Apr 11.

[20] P.J. Saylor, R.J. Lee, K.S. Arora, et al., Branched chain RNA In situ hybridization for androgen receptor splice variant AR-V7 as a prognostic biomarker for metastatic castration-sensitive prostate cancer, Clin. Cancer Res. 23 (2) (2017) 363–369, https://doi.org/10.1158/1078-0432.CCR-16-0237. Jan 15.

[21] J.N. Eskra, D. Rabizadeh, J. Zhang, W.B. Isaacs, J. Luo, C.P. Pavlovich, Specific detection of prostate cancer cells in urine by RNA In situ hybridization, J. Urol. 206 (1) (2021) 37–43, https://doi.org/10.1097/JU.0000000000001691. Jul.

[22] J.I. Warrick, S.A. Tomlins, S.L. Carskadon, et al., Evaluation of tissue PCA3 expression in prostate cancer by RNA in situ hybridization–a correlative study with urine PCA3 and TMPRSS2-ERG, Mod. Pathol. 27 (4) (2014) 609–620, https://doi.org/10.1038/modpathol.2013.169. Apr.

[23] R. Mehra, A.M. Udager, T.U. Ahearn, et al., Overexpression of the long non-coding RNA SChLAP1 independently predicts lethal prostate cancer, Eur. Urol. 70 (4) (2016) 549–552, https://doi.org/10.1016/j.eururo.2015.12.003. Oct.

[24] S. Jamalzadeh, A. Hakkinen, N. Andersson, et al., QuantISH: RNA in situ hybridization image analysis framework for quantifying cell type-specific target RNA expression and variability, Lab. Invest. 102 (7) (2022) 753–761, https://doi.org/10.1038/s41374-022-00743-5. Jul.

[25] X. Xi, T. Li, Y. Huang, et al., RNA biomarkers: frontier of precision medicine for cancer, Noncoding. RNa 3 (1) (2017), https://doi.org/10.3390/ncrna3010009. Feb 20.

[26] Y. Liu, A. Beyer, R. Aebersold, On the dependency of cellular protein levels on mRNA abundance, Cell 165 (3) (2016) 535–550, https://doi.org/10.1016/j.cell.2016.03.014. Apr 21.

[27] E. Lundberg, L. Fagerberg, D. Klevebring, et al., Defining the transcriptome and proteome in three functionally different human cell lines, Mol. Syst. Biol. 6 (2010) 450, https://doi.org/10.1038/msb.2010.106. Dec 21.

[28] A. Macklin, S. Khan, T. Kislinger, Recent advances in mass spectrometry based clinical proteomics: applications to cancer research, Clin. Proteomics. 17 (2020) 17, https://doi.org/10.1186/s12014-020-09283-w.

[29] N. Momenbeitollahi, T. Cloet, H. Li, Pushing the detection limits: strategies towards highly sensitive optical-based protein detection, Anal. Bioanal. Chem. 413 (24) (2021) 5995–6011, https://doi.org/10.1007/s00216-021-03566-3. Oct.

[30] B. Schwanhausser, D. Busse, N. Li, et al., Global quantification of mammalian gene expression control, Nature 473 (7347) (2011) 337–342, https://doi.org/10.1038/nature10098. May 19.

[31] C. Vogel, E.M. Marcotte, Insights into the regulation of protein abundance from proteomic and transcriptomic analyses, Nat. Rev. Genet. 13 (4) (2012) 227–232, https://doi.org/10.1038/nrg3185. Mar 13.

[32] R. Schindler, B.D. Clark, C.A. Dinarello, Dissociation between interleukin-1 beta mRNA and protein synthesis in human peripheral blood mononuclear cells, J. Biol. Chem. 265 (18) (1990) 10232–10237. Jun 25.

[33] F. Wang, J. Flanagan, N. Su, et al., RNAscope: a novel in situ RNA analysis platform for formalin-fixed, paraffin-embedded tissues, J. Mol. Diagn. 14 (1) (2012) 22–29, https://doi.org/10.1016/j.jmoldx.2011.08.002. Jan.